Use of Attenuated Total Reflection Infrared Spectroscopy for Analysis of Partitioning of Solutes between Thin Films and Solution

ARTICLE *in* ANALYTICAL CHEMISTRY · OCTOBER 2005

Impact Factor: 5.64 · DOI: 10.1021/ac050689w · Source: PubMed

2 AUTHORS, INCLUDING:

Viatcheslav Freger
Technion - Israel Institute of Technology
77 PUBLICATIONS **2,096** CITATIONS

Anal. Chem. **2005,** *77,* 6019−6025

Use of Attenuated Total Reflection Infrared Spectroscopy for Analysis of Partitioning of Solutes between Thin Films and Solution

Viatcheslav Freger* and Adi Ben-David

Zuckerberg Institute for Water Research and Department of Biotechnology and Environmental Engineering, Ben-Gurion University of the Negev, POB 635, Beer-Sheva 84105, Israel

The paper examines attenuated total reflection (ATR) spectroscopy as a tool for quantifying the partitioning of small molecular species between a solution and a thin film, while the film is directly exposed to the solution for equilibration. For the case of a thin film having a thickness substantially smaller than the decay length of the evanescent wave, we developed suitable linear relationships that relate the measured absorption of the characteristic band to the concentration of the species under study in the film and in solution. In the application of ATR-Fourier transform infrared spectroscopy, the method is particularly suitable for films a few tens to hundreds of nanometers thick and for solutes that preferentially partition into the film. As an example, the partitioning isotherm of 1-pentanol between water and a thin polyamide film separated from a reverse osmosis membrane was determined experimentally, and the limitations of the method are discussed.

Attenuated total reflection spectroscopy (ATR), particularly Fourier transform infrared version (ATR-FT-IR), has become a routine technique for the study of thin films, powders, surface layers of bulk materials, and strongly absorbing solutions.[1−3] Since IR spectroscopy readily distinguishes between different molecular species by focusing on specific bands, it may be utilized for quantifying relative amounts of different species in different phases. The applications of ATR-FT-IR cover a wide range of subjects, including surface modification[4] and degradation,[5] self-assembled thin films,[6] grafted polymer layers,[7] adsorption phenomena,[8] electrochemistry,[9] and biological[10] and synthetic[11] membranes. Most of the applications apply the method for qualitative and semiquantitative analyses of compositional changes,[4−11] conformation,[12] orientation,[1,3,13] and molecular interactions[14] in thin layers attached to an ATR crystal with a high index of refraction. Quantitative studies are not common, even though the potential of ATR-FT-IR as a technique for quantitative analysis of thin films has been successfully demonstrated in a number of studies.[1−3,15] The main obstacles to the more widespread use of the technique are the nonuniform distribution of the field intensity inside the film and the adjacent bulk material and the need to account separately for the three differently polarized components of the

* To whom correspondence should be addressed. E-mail: vfreger@bgu.ac.il.

(1) Harrick, N. J. *Internal Reflection Spectroscopy*; Interscience Publishers: New York, 1967.
(2) Mirabella, F. M. In *Internal Reflection Spectroscopy Theory and Applications*; Mirabella, F. M., Ed.; Marcel Dekker: New York, 1993.
(3) Urban, M. W. *Attenuated Total Reflectance Spectroscopy of Polymers: Theory and Practice*; American Chemical Society: Washington, DC, 1996.
(4) Lehockýa, M.; Drnovskáa, H.; Lapíková, B.; Barros-Timmons, A. M.; Trindade, T.; Zembalac M.; Lapík, L. *Colloids Surf., A* **2003**, *222*, 125−131. Zhang, J.; Yuan, Y. L.; Wu, K. H.; Shen J.; Lin S. C. *Colloids Surf., B* **2003**, *28*, 1−9. Mao, C.; Qiu, Y. Z.; Sang, H. B.; Mei, H.; Zhu, A. P.; Shen, J.; Lin, S. C. *Adv. Colloid Interface Sci.* **2004**, *110*, 5−17. Janorkar, A. V.; Metters, A. T.; Hirt, D. E. *Macromolecules* **2004**, *37*, 9151−9159.
(5) Mitra, S.; Ghanbari-Siahkali, A.; Kingshott, P.; Hvilsted, S.; Almdal, K. *J. Polym. Sci., Part A: Polym. Chem.* **2004**, *42*, 6216−6229. Kiwi, J.; Nadtochenko, V. *J. Phys. Chem. B* **2004**, *108*, 17675−17684. Frydman, E.; Cohen, H.; Maoz, R.; Sagiv, J. *Langmuir* **1997**, *13*, 5089−5106. Bokria, J. G.; Schlick, S. *Polymer* **2002**, *43*, 3239−3246.
(6) Baptiste, A.; Gibaud, A.; Bardeau, J. F.; Wen, K.; Maoz, R.; Sagiv, J.; Ocko, B. M. *Langmuir* **2002**, *18*, 3916−3922. Gershevitz, O.; Sukenik, C. N. *J. Am. Chem. Soc.* **2004**, *126*, 482−483.
(7) Korematsu, A.; Takemoto, Y.; Nakaya. T.; Inoue, H. *Biomaterials* **2002**, *23*, 263−271. Boyes, S. G.; Brittain, W. J.; Weng, X.; Cheng, S. Z. D. *Macromolecules* **2002**, *35*, 4960−4967. Granville, A. M.; Boyes, S. G.; Akgun, B.; Foster, M. D.; Brittain, W. J. *Macromolecules* **2004**, *37*, 2790−2796. Tomita, T.; Li, Y. J.; Nakaya, T. *Chem. Mater* **1999**, *11*, 2155−2162, Sukhishvili, S. A.; Granick, S. *Langmuir* **1997**, *13*, 4935−4938.
(8) Jacobsen, R. J.; Strand, S. W. In *Internal Reflection Spectroscopy: Theory and Applications*; Mirabella, F. M., Ed.; Marcel Dekker: New York, 1993. Chabal, Y. J. In *Internal Reflection Spectroscopy: Theory and Applications*; Mirabella, F. M., Ed.; Marcel Dekker: New York, 1993. Sethuraman, A.; Belfort G. *Biophys. J.* **2005**, *88*, 1322−1333. Al-Hosney, H. A.; Grassian, V. H. *Phys. Chem. Chem. Phys.* **2005**, *7*, 1266−1276. Li, H. Y.; Tripp, C. P. *J. Phys. Chem. B* **2004**, *108*, 18318−18326. Mueller, M.; Kessler, B.; Adler, H. J.; Lunkwitz, K. *Macromol. Symp.* **2004**, *210*, 157−164.
(9) Bauhofer, J. In *Internal Reflection Spectroscopy: Theory and Applications*; Mirabella, F. M., Ed.; Marcel Dekker: New York, 1993. Moon, S. M.; Bock, C.; MacDougall, B. *J. Electroanal. Chem.* **2004**, *568*, 225−233. Wang, S. F.; Du, D. *Anal. Lett.* **2004**, *37*, 361−375.
(10) Fringeli, U. P. In *Internal Reflection Spectroscopy: Theory and Applications*; Mirabella, F. M., Ed.; Marcel Dekker: New York, 1993. Jiang, C. H.; Gamarnik, A.; Tripp, C. P. *J. Phys. Chem.* **2005**, *109*, 4539−4544. Mangoni, M. L.; Papo, N.; Mignogna, G.; Andreu, D.; Shai, Y.; Barra, D.; Simmaco, M. *Biochemistry* **2003**, *42*, 14023−14035.
(11) Belfer, S.; Purinson, Y.; Kedem, O. *Acta Polym.* **1998**, *49*, 574−582. Freger, V.; Gilron, J.; Belfer, S. *J. Membr. Sci.* **2002**, *209*, 283−292. Vico, S.; Palys, B.; Buess-Herman, C. *Langmuir* **2003**, *19*, 3282−3287. Ulbricht, M.; Richau, K.; Kamusewitz, H. *Colloid Surf., A* **1998**, *138*, 353−366. Han, M.; Sethuraman, A.; Kane, R. S.; Belfort, G. *Langmuir* **2003**, *19*, 9868−9872.
(12) Tretinnikov, O. N.; Ohta, K. *Macromolecules* **2002**, *35*, 7343−7353.
(13) Shin, E. M.; Koenig, J. L. *Appl. Spectrosc.* **2002**, *56*, 1251−1258.
(14) Sammon, C.; Deng, C. S.; Yarwood, J. *Polymer* **2003**, *44*, 2669−2677. Kharlampieva, E.; Sukhishvili, S. A. *Langmuir* **2004**, *20*, 9677−9685.
(15) Tompkins, H. G. *Appl. Spectrosc.* **1974**, *28*, 335−341. Iwamoto, R.; Ohta, K. *Appl. Spectrosc.* **1984**, *38*, 359−365. Mirabella, F. M. *J. Polym. Sci., Polym. Phys. Ed.* **1985**, *23*, 861−871.

10.1021/ac050689w CCC: $30.25
Published on Web 08/11/2005

incident IR beam.[1,2] (An additional complication comprises the spectral distortions originating from the wavelength dependence of the field intensity and from optical dispersion effects near strong bands, but these may be overcome by applying special correction algorithms[3] or simply by choosing specific bands with minimal overlap with other bands in the spectrum.) However, the spatial nonuniformity of the evanescent field may actually be exploited as an advantage and has indeed been utilized in applications such as depth profiling,[2,3,16] the determination of diffusivity of solutes in polymers,[17] and the analysis of the molecular transport and kinetics of surface binding of probe molecules in thin porous films.[18] This paper analyzes a previously unexplored potential application of ATR, namely, determination of the partitioning of small molecules between a thin film and a bulk solution.

Unlike previous ATR studies of partitioning and transport in thin films (e.g., refs 17 and 18), in which *relative* changes of the solute concentrations in the film were measured and employed in subsequent calculations, in this study we looked at how the technique could be applied to directly determine the *absolute* amount of a solute in a film. Our motivation was the need to quantify partitioning in thin polyamide films that form the selective layer of the modern reverse osmosis membranes used for pressure-driven separation (filtration) of solutes from water. Unexpectedly, the high passage of certain organic solutes through these membranes was inconsistent with the conventional exclusion-by-size picture, and it was assumed that differences in thermodynamic affinity toward polyamide, i.e., partitioning, might be responsible for the phenomenon (e.g., see ref 19 and references therein). Unfortunately, these thin (<0.3 μm) polyamide membranes are made in situ by interfacial polymerization on a porous support and cannot be prepared as bulk samples, which precludes the use of traditional approaches for partitioning measurements. Another difficulty is that partitioning must be measured under conditions corresponding to those in which the membranes operate, i.e., upon exposure to aqueous solutions. In this respect, ATR offers a nearly ideal arrangement, whereby the film may be directly exposed to a bulk solution for equilibration and the IR absorption by the film is maximized due to multiple reflections and to the fact that the field intensity is greatest in the film. In this study, we exploited a recently developed procedure that allows isolation and transfer of the polyamide films from a commercial membrane to a solid substrate such as an ATR element.[20]

Selective partitioning from solution to a thin polymeric film that coats an ATR element is also employed in environmental analysis of organic pollutants in aqueous media (for increasing sensitivity to certain solutes and reducing interference from other components present in solution).[21] The relationships developed in this study may directly apply to such work. They can also be useful in studies of thin films such as biological membranes and self-assembled layers. As is the case for the polyamide films studied in this work, many of the above-described structures do not exist as bulk samples amenable to classic quantitative analytical techniques and are often too thin to produce sufficient intensities in the IR transmission mode, particularly for measurements of the partitioning of a dilute species.

The general analytical solution for the distribution of field intensities in a planar stratified medium was given by Hansen,[22] but it is too cumbersome to apply in its general form. Compact solutions are known for the limiting cases of very thin and very thick planar films.[23] For intermediate thicknesses, Iwamoto and Ohta developed analytical relationships by assuming the same refractive index for the film and the bulk medium.[24] They demonstrated that bands of the film and of the bulk medium may both be utilized for measuring film thickness. Recently, Yang et al.[25] showed how a similar linearized formula could be used for determining the thickness of an optically nonadsorbing film from attenuation of a band of the adjacent bulk. For arbitrary values of optical parameters of the film and the substrate, Urban[3] proposed a semiempirical interpolation formula that connects the exact solutions for absorption by very thin and thick films.

The existing relationships usually aim at work with only one medium, either a film or a substrate, for which calibration of the specific absorptivity (per unit thickness or concentration) is required. The calibrated specific absorptivity implicitly includes a constant factor that accounts for the relative amplitude of the evanescent field in the relevant phase. However, in the case of partitioning measurements, two phases are involved (unless the partitioning is highly selective), and one must account for the differences in the above-mentioned factor for the two phases. For this purpose, suitable and fairly simple linearized relationships were developed and analyzed in this work for films of small (submicrometer) thickness. In the limiting case of an infinite partitioning coefficient (zero solubility in the bulk), the formulas become equivalent to the well-known thin-film solution.[1−3,23] In this respect, the result may be viewed as a generalization of the thin-film formulas for finite partitioning coefficients.

THEORY

Linearized Relationships for ATR Absorbance. We consider the case of a homogeneous planar layer of thickness h (medium 2), which is placed between an ATR crystal (medium 1) and a solution (medium 3). The incident beam hits the 1−2 interface from the 1 side at incidence angle θ. Assuming weak absorption, all indices of refraction n_j (j = 1, 2, 3) may be viewed as real numbers. At a specific frequency, media 2 and 3 are assigned absorptivities that may be written as $\epsilon_j C_j$, where ϵ_j and C_j are, respectively, the specific, e.g., molar, absorption coefficient and molar concentration of the component of interest in medium j. The total absorptivity should actually be added up for all components, yet we assume the other contributions to be subtracted with the background.

(16) Fina, L. J.; Chen, G. C. *Vib. Spectrosc.* **1991**, *1*, 353−361.
(17) Fieldson, G. T.; Barbari, T. A. *Polymer* **1993**, *34*, 1146−1153. Eaton, P.; Holmes, P. A.; Yarwood, J. *Appl. Spectrosc.* **2000**, *54*, 508−516.
(18) Rivera, D.; Harris, J. M. *Anal. Chem.* **2001**, *73*, 411−423.
(19) Nghiem, L. D.; Schaefer, A.; Elimelech, M. *Environ. Sci. Technol.* **2004**, *38*, 1888.
(20) Freger, V. *Environ. Sci. Technol.* **2004**, *38*, 3168.
(21) Visser, T. In *Encyclopedia of Analytical Chemistry: Applications, Theory, and Instrumentation*; Meyers, R. A., Ed.; John Wiley & Sons: Chichester, U.K., 2000. Karlowatz, M.; Kraft, M.; Mizaikoff, M. *Anal. Chem.* **2004**, *76*, 2643−2648.
(22) Hansen, W. N. *J. Opt. Soc. Am.* **1968**, *58*, 380−390.
(23) Harrick, N. J. *J. Opt. Soc. Am.* **1965**, *55*, 851−857.
(24) Iwamoto, R.; Ohta, K. *Appl. Spectrosc.* **1985**, *39*, 418−425.
(25) Yang, P.; Meng, X. F.; Zhang, Z. Y.; Jing, B. X.; Yuan, J.; Yang, W. T. *Anal. Chem.* **2005**, *77*, 1068−74.

By generalizing the formula given by Harrick,[23] the adsorption per reflection may be written as follows:

$$A(h) = \frac{1}{n_1 \cos\theta}\int_0^\infty \langle E(z,h)^2\rangle n_j \epsilon_j C_j \, dz = \frac{n_2}{n_1}\frac{\epsilon_2 C_2}{\cos\theta}\int_0^h \langle E_2{}^2(z,h)\rangle \, dz + \frac{n_3}{n_1}\frac{\epsilon_3 C_3}{\cos\theta}\int_h^\infty \langle E_3{}^2(z,h)\rangle \, dz \quad (1)$$

where $\langle E_j^2(z,h)\rangle$ is the time-averaged square amplitude (intensity) of the field in the medium j at a distance z from the crystal−film (1−2) interface normalized to the intensity of the incident wave and for a specified thickness of the film the h, which is viewed as a parameter. For calculating the integrals, $\langle E_j^2(z,h)\rangle$ must be known for each medium. In general, it is necessary to separately consider the relationships for the three components of the electric field: the component perpendicular to the plane of incidence (E_y or $E_\perp$) and the two components parallel to the plane of incidence, one of which is parallel ($E_{\parallel x}$) and the other is normal ($E_{\parallel z}$) to the interface. The general formulas for the dependence of the three amplitudes on z in all media were given by Hansen,[22] and the formulas used below are derived from his result for a specific case of weak absorbance when n are real and magnetic permeability is equal to 1 for all the phases.

We note first that there is no reflected wave in medium 3; therefore, the squared amplitude decays exponentially in the solution as $\langle E_3^2(z,h)\rangle = \langle E_3^2(h,h)\rangle \exp(-2(z-h)/d_{p3})$, where $\langle E_3^2(h,h)\rangle$ is the intensity of the field that reaches the solution after penetrating the film and d_{p3} is the characteristic depth of penetration (decay length) in the solution, given by[1,2]

$$d_{p3} = \frac{\lambda}{2\pi(n_1{}^2 \sin^2\theta - n_3{}^2)^{1/2}} \quad (2)$$

This turns the second integral in eq 1 into

$$\frac{n_3}{n_1}\frac{\epsilon_3 C_3}{\cos\theta}\int_h^\infty \langle E_3{}^2(z,h)\rangle \, dz = \frac{n_3}{n_1}\frac{\epsilon_3 C_3}{\cos\theta}\frac{d_{p3}}{2}\langle E_3{}^2(h,h)\rangle \quad (3)$$

Second, the problem may be simplified by linearizing the formulas (separately for each polarization) with respect to the parameter h, i.e., approximating them as

$$\langle E^2(z,h)\rangle \approx \langle E^2(z,0)\rangle + h\left.\frac{\partial\langle E^2(z,h)\rangle}{\partial h}\right|_{h=0} \quad (4)$$

If h is small, we may assume that $\langle E_2^2\rangle$ is constant in medium 2 and approximate the first integral in eq 1 as $h\langle E_2{}^2(0,0)\rangle$. This is equivalent to dropping the term linear in z, which amounts to ignoring second-order corrections with respect to h in the final result. Equation 1 thus becomes

$$A(h) \approx \frac{n_2}{n_1}\frac{\epsilon_2 C_2}{\cos\theta} h\langle E_2{}^2(0,0)\rangle + \frac{n_3}{n_1}\frac{\epsilon_3 C_3}{\cos\theta}\frac{d_{p3}}{2}\left[\langle E_3{}^2(0,0)\rangle + h\left.\frac{\partial\langle E_3{}^2(z,h)\rangle}{\partial h}\right|_{h=0,z=h}\right] \quad (5)$$

The intensities $\langle E_2^2(0,0)\rangle$ and $\langle E_3^2(0,0)\rangle$ and the derivative in eq 5 have to be found for each polarization. Let us begin with the perpendicular polarization. The intensity $\langle E_{3\perp}{}^2(h,h)\rangle$ may be expressed as[22]

$$\langle E_{3\perp}{}^2(h,h)\rangle = {}^1/_2|t_{E\perp}|^2 \quad (6)$$

where $t_{E\perp}$ is the overall electric transmission coefficient, which is found from the general relationship[22,26]

$$t_{E\perp} = \frac{t_{12}t_{23}e^{-h/d_{p2}}}{1 + r_{12}r_{23}e^{-2h/d_{p2}}} \quad (7)$$

Here, d_{p2} is defined for phase 2 analogously to eq 2, and the transmission and reflection coefficients (respectively, t and r) in eq 7 may be written as follows:[22,26]

$$t_{12} = \frac{2p_1}{p_1 + ip_2'}, \quad r_{12} = \frac{p_1 - ip_2'}{p_1 + ip_2'}, \quad t_{23} = \frac{2p_2'}{p_2' + p_3'}, \quad r_{23} = \frac{p_2' - p_3'}{p_2' + p_3'} \quad (8)$$

where $p_1 = n_1\cos\theta$, $p_2' = (n_1{}^2 \sin{}^2\theta - n_2{}^2)^{1/2}$, $p_3' = (n_1{}^2 \sin{}^2\theta - n_3{}^2)^{1/2}$ and $i = (-1)^{1/2}$. The primed parameters p_j' designate the imaginary part of the complex parameters $p_j = n_j\cos\theta_j$, where θ_j is the complex angle of incidence or refraction in phase j. For a propagating wave p_j is real, while for an evanescent wave $p_j = ip_j'$, where p_j' is real. We consider only the case in which p_1 and p_3' are real; i.e., total reflection takes place either at the 1−2 or the 2−3 interface. Assume first that p_2' is also real, i.e., total reflection occurs at the 1−2 interface. Straightforward calculations (see Appendix) show that the ultimate expression for $\langle E_{3\perp}{}^2(h,h)\rangle$ may be linearized with respect to h to yield

$$\langle E_{3\perp}{}^2(h,h)\rangle = \frac{2p_1{}^2}{p_1{}^2 + p_3'{}^2}\left[1 - 2\frac{h}{d_{p3}}\frac{p_1{}^2 + p_2'{}^2}{p_1{}^2 + p_3'{}^2}\right] \quad (9)$$

This immediately yields

$$\langle E_{3\perp}{}^2(0,0)\rangle = \frac{2p_1{}^2}{p_1{}^2 + p_3'{}^2}, \quad \left.\frac{\partial\langle E_{3\perp}{}^2(z,h)\rangle}{\partial h}\right|_{h=0,z=0} = -2\langle E_{3\perp}{}^2(0,0)\rangle\frac{1}{d_{p3}}\frac{p_1{}^2 + p_2'{}^2}{p_1{}^2 + p_3'{}^2} \quad (10)$$

The corresponding expressions for the parallel polarization may be obtained from the equation[19]

$$\langle E_{3\parallel}{}^2(h,h)\rangle = {}^1/_2|t_{H\parallel}|^2\frac{n_1{}^2}{n_3{}^2} \quad (11)$$

where the magnetic transmission coefficient $t_{H\parallel}$ may be immediately obtained by replacing $t_{E\perp}$ with $t_{H\parallel}$ in eq 7 and p_j with

(26) Born, M.; Wolf, E. *Principles of Optics*; Pergamon Press: New York, 1975.

p_j/n_j^2 in eq 8 for the transmission and reflection coefficients, respectively, for perpendicular polarization. This means that eqs 9 and 10 are converted to the corresponding equations for parallel polarization simply by changing all p_j to p_j/n_j^2 and multiplying the whole expression by n_1^2/n_3^2. Thus, for instance,

$$\langle E_{3||}{}^2(0,0)\rangle = \frac{n_1{}^2}{n_3{}^2}\frac{2p_1{}^2/n_1{}^4}{p_1{}^2/n_1{}^4 + p_3'^2/n_3{}^4} \tag{12}$$

which is further split into x and z components as

$$\langle E_{3||x}{}^2(0,0)\rangle = \frac{p_3'^2}{n_3{}^2}\frac{2p_1{}^2/n_1{}^4}{p_1{}^2/n_1{}^4 + p_3'^2/n_3{}^4} \tag{13a}$$

$$\langle E_{3||z}{}^2(0,0)\rangle = \frac{n_1{}^2\sin{}^2\theta}{n_3{}^2}\frac{2p_1{}^2/n_1{}^4}{p_1{}^2/n_1{}^4 + p_3'^2/n_3{}^4} \tag{13b}$$

The intensities for medium 2 are found from the continuity of the field intensity for the x and y components and from the continuity of the electric displacement for z:

$$\langle E_{2\perp}{}^2(0,0)\rangle = \langle E_{3\perp}{}^2(0,0)\rangle,\ \langle E_{2||x}{}^2(0,0)\rangle = \langle E_{3||x}{}^2(0,0)\rangle,\ \langle E_{2||z}{}^2(0,0)\rangle = \langle E_{3||z}{}^2(0,0)\rangle\frac{n_3{}^4}{n_2{}^4} \tag{14}$$

The resulting expressions for the absorbance per reflection are

$$A_\perp = A_y = \frac{2p_1}{p_1{}^2 + p_3'^2}\left[\epsilon_3 C_3 n_3\left(\frac{d_{p3}}{2} - h\frac{p_1{}^2 + p_2'^2}{p_1{}^2 + p_3'^2}\right) + \epsilon_2 n_2 C_2 h\right]$$

$$A_{||x} = A_x = \frac{2p_1 p_3'^2/n_1{}^2}{p_1{}^2 n_3{}^4/n_1{}^4 + p_3'^2}\left[\epsilon_3 C_3 n_3\left(\frac{d_{p3}}{2} - h\frac{p_1{}^2/n_1{}^4 + p_2'^2/n_2{}^4}{p_1{}^2/n_1{}^4 + p_3'^2/n_3{}^4}\right) + \epsilon_2 C_2 n_2 h\right]$$

$$A_{||z} = A_z = \frac{2p_1\sin{}^2\theta}{p_1{}^2 n_3{}^4/n_1{}^4 + p_3'^2}\left[\epsilon_3 C_3 n_3\left(\frac{d_{p3}}{2} - h\frac{p_1{}^2/n_1{}^4 + p_2'^2/n_2{}^4}{p_1{}^2/n_1{}^4 + p_3'^2/n_3{}^4}\right) + \epsilon_2 C_2 n_2 h\frac{n_3{}^4}{n_2{}^4}\right] \tag{15}$$

When p_2 is real, i.e., the actual total reflection takes place at the 2−3 interface, p_2 replaces ip_2' in eq 8, and the relationships 15 are slightly modified to become

$$A_\perp = A_y = \frac{2p_1}{p_1{}^2 + p_3'^2}\left[\epsilon_3 C_3 n_3\left(\frac{d_{p3}}{2} - h\frac{p_1{}^2 - p_2{}^2}{p_1{}^2 + p_3'^2}\right) + \epsilon_2 C_2 n_2 h\right]$$

$$A_{||x} = A_x = \frac{2p_1 p_3'^2/n_1{}^2}{p_1{}^2 n_3{}^4/n_1{}^4 + p_3'^2}\left[\epsilon_3 C_3 n_3\left(\frac{d_{p3}}{2} - h\frac{p_1{}^2/n_1{}^4 - p_2{}^2/n_2{}^4}{p_1{}^2/n_1{}^4 + p_3'^2/n_3{}^4}\right) + \epsilon_2 C_2 n_2 h\right]$$

$$A_{||z} = A_z = \frac{2p_1\sin{}^2\theta}{p_1{}^2 n_3{}^4/n_1{}^4 + p_3'^2}\left[\epsilon_3 C_3 n_3\left(\frac{d_{p3}}{2} - h\frac{p_1{}^2/n_1{}^4 - p_2{}^2/n_2{}^4}{p_1{}^2/n_1{}^4 + p_3'^2/n_3{}^4}\right) + \epsilon_2 C_2 n_2 h\frac{n_3{}^4}{n_2{}^4}\right] \tag{16}$$

Obviously, eqs 15 and 16 coincide when $p_2 = p_2' = 0$, i.e., at the critical angle (transition between refraction and total reflection at the 1−2 interface).

The total measured absorbance (decimal logarithm-based) is related to the absorbances of the components given by eq 15 or 16 by means of a nonlinear relationship:

$$A = \log(I_{\perp 0} + I_{||0}) - \log(10^{-NA_\perp} I_{\perp 0} + 10^{-N(A_{||x}+A_{||z})} I_{||0}) \tag{17}$$

where I_0 designates the initial intensities for the corresponding polarizations and N is the number of reflections. If the total absorbance is small, about $A \le 0.5$,[24] which is most often the case, then eq 17 is well approximated by a linear relationship:[24]

$$A \approx N\left(\frac{I_{\perp 0}}{I_{\perp 0} + I_{||0}}A_\perp + \frac{I_{\perp 0}}{I_{\perp 0} + I_{||0}}(A_{||x} + A_{||z})\right) \tag{18}$$

For a homogeneous film, all parameters in relationships 15, 16, and 18 are constant, and they may be condensed into a simple linear relationship between the measured absorbance and the concentration of the relevant species in the bulk and film phases:

$$A = a\epsilon_3 C_3(1 - b + d(\epsilon_2/\epsilon_3)K) \tag{19}$$

where $K = C_2/C_3$ is the sought partitioning coefficient. The parameter a depends on the characteristics of the instrument (N and polarization), of the crystal and of the solution but is not dependent on the film. The product $a\epsilon_3$ is easily determined from ATR experiments with a crystal directly exposed to solution; i.e., for $h = 0$. The parameters b and d depend on the optical characteristics of all three phases, and in the linear limit, $h/d_{p3} \ll 1$ are proportional to the ratio h/d_{p3}, i.e., to the film thickness. They express, respectively, the relative decrease in absorbance by the solution (bulk absorbance) due to the presence of the film (the second term in brackets) and the relative increase in absorbance due to the partitioning of the solute into the film (the third term). The use of this equation for quantifying sorption or partitioning of a molecular species between the bulk and a thin film requires knowledge of: the thickness of the film, the refractive indices of all three phases, and the ratio of the extinction coefficients of the solute in the film and in the bulk ϵ_2/ϵ_3. The thickness and refractive index of the film are in principle accessible, even in solution, e.g., by ellipsometry. However, determination of the ϵ_2/ϵ_3 ratio might present certain difficulties as is discussed in the next section.

Extinction Coefficient in the Film. It is usually difficult or impossible to determine the concentration of a solute inside a thin film, unless the film may be prepared as a thick bulk sample amenable to standard partitioning measurements that can subsequently be used to "calibrate" the ATR data. For this reason, it is often not possible to experimentally determine the extinction coefficient of a solute in a film as can be done for the extinction coefficient of the solute in solution.

The problem might be resolved by using an appropriate theoretical model to assess the extinction coefficient of the film from the other data. For instance, we may use the relationship

between the extinction coefficient and the imaginary part of the complex refractive index of the medium $\hat{n} = n + ki$ by[2,26]

$$\epsilon C = \frac{4\pi \, \mathrm{Im}(\hat{n})}{\lambda} = \frac{4\pi k}{\lambda} \tag{20}$$

and the Maxwell−Garnett formula[27] to estimate the refractive index of a two-component mixture consisting of a matrix (treated as one component) and a dilute solute. A similar approach based on the Lorenz−Lorentz relationships has been described by Müller and Abraham-Fuchs.[28] The Maxwell−Garnett formula may be written as

$$\frac{\hat{n} - \hat{n}_\mathrm{m}}{\hat{n} + 2\hat{n}_\mathrm{m}} = C\frac{\hat{n}_\mathrm{s} - \hat{n}_\mathrm{m}}{\hat{n}_\mathrm{s} + 2\hat{n}_\mathrm{m}} \tag{21}$$

where $\hat{n}_\mathrm{m}$ and $\hat{n}_\mathrm{s}$ are the complex refractive indices of the matrix and solute and C is the concentration of the solute expressed as the volume fraction. Equation 21 may be replaced by other relationhips, e.g., the Bruggeman formula,[27] but it is usually the equation of choice for dilute systems. To simplify the calculations, we recall that the imaginary part of all $\hat{n}$ is small, i.e., $k \ll n$ (weak absorption limit). If we focus on a sufficiently strong band specific to the solute of interest, we may neglect the imaginary component of $\hat{n}_\mathrm{m}$. By solving eq 21 for $\hat{n}$, isolating the imaginary part, and substituting it into eq 20, we obtain for the volume fraction-related extinction coefficient

$$\epsilon = \frac{36\pi}{\lambda} k_s \frac{n_\mathrm{s}/n_\mathrm{m}}{[(n_\mathrm{s}/n_\mathrm{m})^2 + 2]^2} \tag{22}$$

To obtain the molar extinction coefficient, eq 22 should be multiplied by the molar volume of the solute. Equation 22 suggests that for the same band

$$\frac{\epsilon_2}{\epsilon_3} = \frac{n_3}{n_2}\left[\frac{(n_\mathrm{s}/n_3)^2 + 2}{(n_\mathrm{s}/n_2)^2 + 2}\right]^2 \tag{23}$$

The only unknown parameter n_s may be taken as that of a pure liquid solute or estimated using suitable structure−property correlations directly[29] or from the electronic polarizability.[30] However, in most practical cases, the refractive indices of liquids and organic solids are confined to a fairly limited range, approximately between 1.3 and 1.7,[31] thus both n_s/n_2 and n_s/n_3 are not expected to change beyond the range $0.75 < n_\mathrm{s}/n_\mathrm{m} < 1.3$. This inequality—in conjunction with eq 23—suggests that ϵ_2 and ϵ_3 will differ by no more than 25%. For many practical purposes, the simple assumption that $\epsilon_2 \approx \epsilon_3$ could be fairly satisfactory, as long as the particular band is weakly affected by strong specific interactions with the environment, such as protonation, strong hydrogen bonding, film anisotropy, or molecular orientation, that might modify the position and intrinsic intensity of the relevant band.

EXPERIMENTAL SECTION

The procedures for the preparation of polyamide films and the assessment of their characteristics are described in detail elsewhere.[20,32] Briefly, the polyamide film was separated from a commercial ESPA1 membrane (kindly supplied by Dr. Mark Wilf, Hydranautics) and attached to a ZnSe ATR element (incident angle 45° and 6 nominal reflections) by careful dissolution of the supporting polysulfone film in organic solvents. The ATR crystal formed the bottom of a trough cell of a Gateway ATR assembly (Specac), which was then mounted in the spectrometer and filled with the appropriate solutions. The spectra were recorded on an Impact 410 FT-IR spectrometer (Nicolet) using a nonpolarized beam. For each sample (either a bare crystal or a polyamide-coated element), the spectrum of pure water was taken first and used then as the background. The measurements for each sample were carried out for solutions of four to six different concentrations. The reproducibility was checked by using three to four similarly prepared samples.

The thickness of the dry film placed on a silicon wafer was determined from the intensity of the band of carbon relative to the band of silicon in an energy-dispersion spectrum (EDS) [Quanta 200 scanning electron microscope (JEOL)].[32] The intensity of the carbon band was calibrated by using three different polystyrene films spin-coated onto the same substrate, whose thickness had been determined by elliposmetry. A good linear relationship was found between the intensity of the relevant EDS band and the film thickness of the polystyrene film. The thickness of the polyamide films (averaged over ~1-mm^2 area) was in good agreement with AFM and TEM observations. The swelling of the films was determined by AFM (Dimension 3100, Veeco-Digital Instruments), as described in ref 20. The refractive index of the dry film was estimated using appropriate structure−property correlations.[29] Such estimates agreed well with the results of ellipsometry obtained for polyamide films of a slightly different type.[32] The refractive index for swollen films was then calculated from the indices of dry polyamide and water and the degree of swelling by means of the Bruggeman formula.[27]

RESULTS AND DISCUSSION

The example was taken from a recent study of the sorption of a number of organic solutes by the active layer of reverse osmosis and nanofiltration membranes.[32] As mentioned earlier, the current study was motivated by the need to examine the possible contribution of partitioning to the unusually high passage of neutral organic solutes through these membranes. Figure 1 shows the intensity of the 1050-cm^{-1} band (assigned to the C−O stretching in 1-pentanol) for film-free and film-covered crystals as a function of the 1-pentanol concentration in solution. The 1050-cm^{-1} band of 1-pentanol was not near any of the significant bands

(27) Landauer, R. In *Proceedings of the First Conference on Electrical Transport and Optical Properties of Inhomogeneous Media*; Garland, J. C., Tanner, D. B., Eds. AIP Conf. Proc. No 40, AIP: New York, 1978.
(28) Müller, G. J.; Abraham-Fuchs, K. In *Internal Reflection Spectroscopy Theory and Applications*; Mirabella, F. M. Ed.; M. Dekker: New York, 1993.
(29) Van Krevelen, D. W.; Hoftyzer, P. J. *Properties of Polymers: Correlation with Chemical Structure*; Elsevier: Amsterdam, The Netherlands, 1972.
(30) Israelashvili, J. *Intermolecular and Surface Forces*; Academic Press: London, 1991.
(31) Lide, D. R., Ed. *Handbook of Chemistry and Physics*, 84th ed.; CRC Press: Boca Raton, FL, 2003.
(32) Ben-David, A.; Bason, S.; Jopp, J.; Oren, Y.; Freger, V. *Environ. Sci. Technol.* submitted.

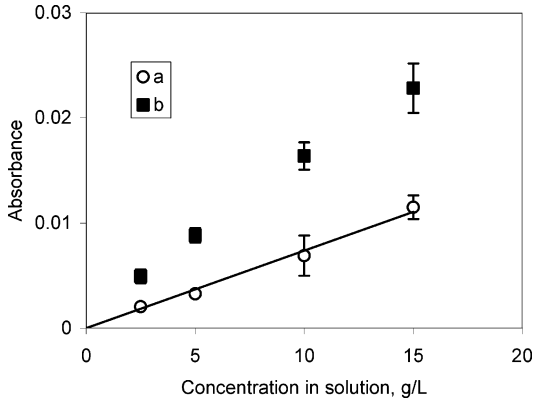

Figure 1. Intensity of the 1050-cm^{-1} band vs concentration of 1-pentanol in aqueous solution. A ZnSe ATR crystal with six nominal reflections and an incidence angle of 45° was used. The symbols represent the absorbance for (a) the bare crystal and (b) the crystal covered with a polyamide film. The solid line is the linear fit to the bare crystal results. The error bars show standard deviations.

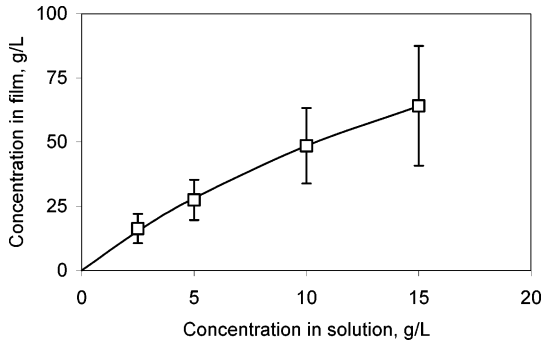

Figure 2. Sorption isotherm of 1-pentanol calculated from the results shown in Figure 1. The symbols represent the calculated results, and the solid line shows a fitted Langmuir isotherm. The error bars show the total error calculated using standard error propagation relationships from the errors of measured absorbances shown in Figure 1.

of water or polyamide, which facilitated determination of the band intensity and minimized spectrum distortions characteristic of ATR.[3] The product $a\epsilon_3$ of eq 19 for 1-pentanol was determined from the slope of the band intensity versus concentration of the alcohol for a bare crystal ($b = d = 0$), while the other optical parameters of the film and solution were evaluated independently as described in the Experimental Section, which allowed calculation of the parameters b and d in eq 19. The following values of the parameters were used in the calculations: $h = 183$ nm, $n_1 = 2.4$, $n_2 = 1.67$ (from $n = 1.70$ for the dry film and swelling 6%), $n_3 = 1.25$ (for wavelength $\lambda = 9.52$ μm), $\theta = 45°$, and $N = 6$.

Assuming $\epsilon_2 \approx \epsilon_3$, it was possible to calculate the partitioning isotherm of 1-pentanol between the film and solution by means of eq 19 (Figure 2). The isotherm shown in Figure 2 appears to be slightly convex. Extrapolation of the isotherm to high dilutions, i.e., to conditions relevant to reverse osmosis experiments, using a Langmuir isotherm yields the partitioning coefficient $K = 6.7$. This and other similar measurements for alcohols smaller than 1-pentanol show that the value of K steadily increases with the molecular size for alcohols larger than propanol, apparently as a result of the rapidly decreasing solubility (or increasing activity coefficient) in water. This finding may indeed explain why the rejection of alcohols larger than propanol by reverse osmosis is surprisingly only weakly dependent on the molecular size, since the effects of size and partitioning approximately cancel each other out.

The adsorption of the solute at the surface of the bare crystal and the film was disregarded in the above-described analysis; this constitutes a potential source of errors. If adsorption is described by a Langmuir isotherm $\Gamma = \Gamma_0 kC/(1 + kC)$, where Γ is the surface excess and Γ_0 and k are parameters, then the error in K is expected to be of the order of $\Delta K \approx \Gamma_0 k/h$. For 1-pentanol at the air−water interface $\Gamma_0 = 6 \times 10^{-6}$ mol/m^2 and $k = 0.023$ m^3/mol,[33] and for $h = 183$ nm, we obtain a relatively large value $\Delta K = 1.5$. The data on pentanol adsorption on the polyamide−water and ZnSe−water interfaces are not available. We may argue, however, that ZnSe is very hydrophilic,[34] while the polyamide film is slightly hydrophobic (the reported contact angle for water ranges from 49° to 60°).[35] The interfacial energy for even more hydrophobic dry Nylon-6,6 polyamide (contact angle 70°) and water is less than 20 mN/m^2 and further decreases upon exposure to water;[36] the thermodynamic driving force for surface adsorption on polyamide is then largely reduced compared to the air−water interface (73 mN/m^2).[37] No significant adsorption is thus expected at the polyamide−water interface. At the hydrophilic ZnSe surface water could even be the preferential sorbate, as was observed for clay surfaces exposed to pentanol−water solutions,[38] in which case the error should never exceed $\Delta K \approx \tau/h$, where τ is the thickness of the surface region. This thickness is of the order of 1 Å for small solutes;[37] thus, the error associated with surface adsorption on ZnSe is expected to be negligible. Since ΔK must depend on h, a convenient test for this type of error can be examination of films of different thicknesses. For two solutes, aniline and hydroquinone, which gave values of K comparable to the value of 1-pentanol, the isotherms were also measured for another membrane, SWC1, which is chemically identical but about half as thin as ESPA1 (average thickness 96 nm). No significant differences between the isotherms were found for these solutes,[32] which strongly suggests that interferences from surface adsorption for the considered solutes and films are indeed small.

It is important to stress the other limitations of the method. Inspection of eq 19 shows that for each equation the quality of the data is governed by the magnitude of the last term in parentheses relative to the other terms. This suggests that the precision will be better for thicker films (large h and hence larger parameters b and d in eq 19) and larger partitioning (large K). For very thick films ($h \sim d_{p2}$ and larger), the linearized relations eq 15 and 16 can no longer be used, and they should be replaced with complex nonlinear equations,[22] which for E_2^2 will have to be integrated over the film thickness (cf. eq 1). Very small partitioning coefficients $K \ll 1$ will be impossible to measure, since the formulas will be insensitive to K (eq 15, 16, or 19). This is perhaps the most serious limitation of the method, which is illustrated in

(33) Fainerman, V. B.; Miller, R. *J. Colloid Interface Sci.* **1996**, *178*, 168−175.
(34) Noble-Luginbuhl, A. R.; Nuzzo, R. G. *Langmuir* **2001**, *17*, 3937−3944. Gun, J.; Sagiv, J. *J. Colloid Interface Sci.* **1986**, *112*, 457−72.
(35) Brant, J. A.; Childress, A. E. *J. Membrane Sci.* **2002**, *203*, 257−273. Gilron, J.; Belfer, S.; Vaisanen, P.; Nystrom, M. *Desalination* **2001**, *140*, 167−179.
(36) Tokoro, T.; Hackam, R. *IEEE Trans. Dielectr. Electron. Insul.* **1999**, *6*, 754−762. Clint, J. H.; Wicks, A. C. *Int. J. Adhes. Adhes.* **2001**, *21*, 267−273.
(37) Adamson, A. W. *Physical Chemistry of Surfaces*, 5th ed.; Wiley-Interscience: New York, 1990.
(38) Dekany, I.; Farkas, A.; Regdon, I.; Klumpp, E.; Narres, H. D.; Schwuger, M. J. *Colloid Polym. Sci.* **1996**, *274*, 981−988.

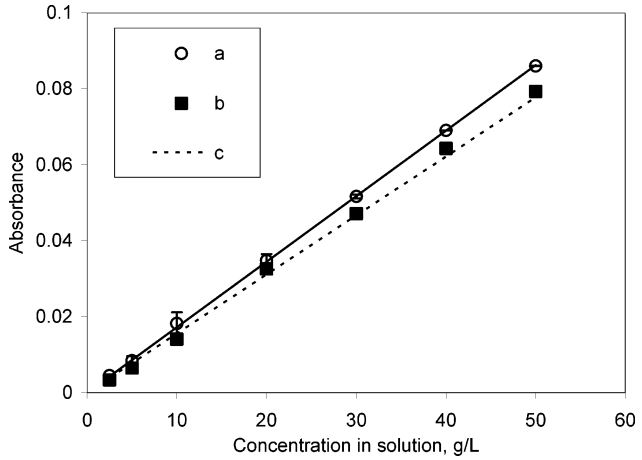

Figure 3. Intensity of the 1084-cm^{-1} band vs concentration of ethylene glycol in aqueous solution: (a) bare crystal and (b) crystal covered with a polyamide film. The solid line is the linear fit to the bare crystal results. The dotted line is the theoretical prediction using eqs 15 and 18 with $K = 0$ and the parameters specified in the text.

the example shown in Figure 3. Here, an attempt was made to measure the sorption of ethylene glycol in a polyamide film, similar to 1-pentanol in Figures 1 and 2. Again, the absorbances for the 1084-cm^{-1} band for different ethylene glycol concentrations lie on a straight line, from which the extinction coefficient is easily estimated. However, an attempt to calculate the partitioning coefficient from measurements with a film-covered crystal led to small and highly scattered values of K. The reason may be seen in Figure 3, in which the dotted line shows the theoretical lower limit calculated using eqs 15 and 18, assuming $K = 0$ and no polarization. The results are too close to the lower limit, and small errors in the measured absorption lead to very large errors in K, with nonphysical negative values being obtained for some points that fall below the dotted line.

Obviously, the method will be inapplicable for films of excessive roughness or heterogeneity. In general, the signal-to-noise ratio should improve for larger ϵ, yet it must be remembered that for very large ϵ, such as that of the OH stretching of water, the assumption of weak absorption $k \ll n$ will be inapplicable.[2,3] Perhaps a better way to control the signal-to-noise ratio and improve sensitivity of the method is to use a larger number of reflections N., e.g., by using a thin crystal, as is often done in studies of self-assembled monolayers.[6] The final recommended improvement is the use of polarized radiation, particularly when the polarization (or absence of polarization) of the incident beam is uncertain. The most convenient choice is perpendicular polarization, for which the intensity of the evanescent field is coupled to the incident intensity in the simplest way, and the calculations are thus simplified.

CONCLUSIONS

This study shows that it is indeed possible to quantify partitioning of solutes between a thin film and solution by means of ATR-FT-IR. For this purpose, simple linearized relationships were developed that are suitable for thin films of small thickness not exceeding a fraction of the penetration depth of the evanescent radiation in the film phase. The presented example shows that the method may be suitable for quantifying high sorption by films of submicrometer thickness (a few tens to hundreds of nanometers). The method offers a convenient nondestructive technique for studying partitioning in thin films within the above restrictions and in the absence of excessive adsorption to the ATR crystal or film surface or strong interactions of the solute with the phases that may lead to large differences in the extinction coefficients of the film and the solution.

ACKNOWLEDGMENT

The authors thank Prof. Yoram Oren, Dr. Sophia Belfer, and Dr. Rosalia Shifrina for informative discussions and Ms. Rosalia Fainshtain for excellent technical assistance in ATR-FT-IR spectroscopy and in preparation of the samples. Financial support from the Israel Ministry of Science (Project 01-01-01496, the Program for Scientific and Technological Development for the Quality of the Environment and Water) is gratefully acknowledged.

APPENDIX. DERIVATION OF EQ 9.

Substitution of eq 8 to eq 7 yields

$$t_{E\perp} = \frac{4p_1p'_2e^{-h/d_{p2}}}{(p_1 + ip'_2)(p'_2 + p'_3) + (p_1 - ip'_2)(p'_2 - p'_3)e^{-2h/d_{p2}}} \quad \text{(A1)}$$

For small h/d_{p2}, the exponents may be expanded as $e^{-h/d_{p2}} \approx 1 - h/d_{p2}$ and $e^{-2h/d_{p2}} \approx 1-2h/d_{p2}$. After collecting the terms proportional to h/d_{p2} in the denominator, we obtain using $(1 - x)/(1 - y) \approx 1 - x + y$ ($x \ll 1$ and $y \ll 1$)

$$t_{E\perp} \approx \frac{2p_1p'_2(1 - h/d_{p2})}{p_1p'_2 + ip'_2p'_3 - (p_1 - ip'_2)(p'_2 - p'_3)h/d_{p2}} \approx \frac{2p_1}{p_1 + ip'_3}\left(1 + \frac{h}{d_{p2}}\left[\frac{(p_1 - ip'_2)(p'_2 - p'_3)}{p'_2(p_1 + ip'_3)} - 1\right]\right) \quad \text{(A2)}$$

Using $(1 + x)(1 + y) \approx 1 + x + y$, we then find the squared absolute value of $t_\perp$ as the product of $t_{E\perp}$ and its complex conjugate

$$|t_{E\perp}|^2 = t_{E\perp}t^*_{E\perp} \approx \frac{4{p_1}^2}{{p_1}^2 + {p'_3}^2}\left(1 + \frac{h}{d_{p2}}\left[\left(\frac{(p_1 + ip'_2)(p'_2 - p'_3)}{p'_2(p_1 - ip'_2)} - 1\right) + \left(\frac{(p_1 - ip'_2)(p'_2 - p'_3)}{p'_2(p_1 + ip'_2)} - 1\right)\right]\right) \quad \text{(A3)}$$

After some rearrangement and noting that $d_{pj} = \lambda/2\pi p'_j$ ($j = 2,3$),

$$|t_{E\perp}|^2 = \frac{4{p_1}^2}{{p_1}^2 + {p'_3}^2}\left[1 - 2\frac{h}{d_{p2}}\frac{p'_3}{p'_2}\frac{{p_1}^2 + {p'_2}^2}{{p_1}^2 + {p'_3}^2}\right] + O([h/d_{p2}]^2) = \frac{4{p_1}^2}{{p_1}^2 + {p'_3}^2}\left[1 - 2\frac{h}{d_{p3}}\frac{{p_1}^2 + {p'_2}^2}{{p_1}^2 + {p'_3}^2}\right] + O([h/d_{p2}]^2) \quad \text{(A4)}$$

from which eq 9 immediately follows.

Received for review April 21, 2005. Accepted June 29, 2005.

AC050689W